

# A new synthetic route to organically capped cadmium selenide nanoparticles†

Oluwatobi Samuel Oluwafemi and Neerish Revaprasadu\*

Received (in Montpellier, France) 30th January 2008, Accepted 5th March 2008

First published as an Advance Article on the web 21st April 2008

DOI: 10.1039/b801717d

We report a novel method for the preparation of monodispersed hexadecylamine (HDA) and tri-*n*-octylphosphine oxide (TOPO) capped CdSe nanoparticles. This route involves the reaction of selenium powder with sodium borohydride (NaBH<sub>4</sub>) to produce selenide ions, followed by the addition of a cadmium salt. The nanoparticles showed quantum confinement with characteristic close to band-edge luminescence in their emission spectra. The nanoparticles were characterised by optical spectroscopy, infrared (IR) spectroscopy, X-ray diffraction (XRD), transmission electron spectroscopy (TEM), and energy dispersive spectroscopy (EDS).

## Introduction

There has been intensive research during the past decade into materials that possess novel electronic properties intermediate between those of macro crystalline solids and molecular entities. These nanostructured materials are capable of self-assembly thereby forming new materials which could potentially transform our technological landscape. Among the various semiconductor nanostructured materials, selenide semiconductors have attracted considerable interest due to their importance in various applications such as thermoelectric cooling materials, optical filters and sensors, optical recording materials, solar cells, superionic materials and laser materials. There are several reported synthetic methods for the preparation of selenide nanoparticles, these include solid-state reactions,<sup>1</sup> solid-state metathesis,<sup>2</sup> self-propagating high temperature synthesis,<sup>3</sup> H<sub>2</sub>Se method,<sup>4</sup> electrochemical methods,<sup>5,6</sup> microwave-assisted methods,<sup>7,8</sup> chemical bath deposition,<sup>9,10</sup> vacuum deposition,<sup>11</sup> and photochemical methods.<sup>12</sup> The use of single and dual source organometallic precursors have also been successfully used to obtain metal selenides.<sup>13–19</sup>

Cadmium selenide is an interesting II–VI semiconductor material because its band gap can be tuned across the visible spectrum by varying the size of the material.<sup>20</sup> Its unique chemical and electronic properties give rise to its potential use in many applications such as biological labels, electronic displays, diodes, lasers, solar cells, and gas sensors.<sup>21</sup> In a landmark paper, Murray *et al.*<sup>13</sup> reported the synthesis of high quality CdSe nanoparticles using tri-*n*-octylphosphine selenide (TOPSe) and dimethyl cadmium [Cd(CH<sub>3</sub>)<sub>2</sub>], in the presence of a coordinating solvent at high temperatures. The latter compound is toxic, unstable, explosive and expensive. Peng's group reported the synthesis of CdSe using CdO as a precursor instead of Cd(CH<sub>3</sub>)<sub>2</sub>.<sup>22</sup> This so called 'green route' proved to be reproducible involving mild and simple reaction conditions,

and could have potential for scaled up industrial applications. O'Brien and co-workers have shown that the diselenocarbamate precursors such as M(Se<sub>2</sub>CNRR')<sub>2</sub>, (M = Cd or Zn) are excellent for the synthesis of air-stable, monodispersed, good quality selenide nanoparticles. A drawback to this route is that the diselenocarbamate ligand is prepared from the toxic and noxious carbon diselenide.<sup>14–16,19,23</sup>

The synthesis of CdSe nanomaterials *via* a solution route appears to be the most simple, cheapest and convenient approach to prepare the selenides in a controlled environment. Selenosulfate and selenourea are the main selenium sources of the Se<sup>2–</sup> ion for the preparation of selenides through reactive solution growth.<sup>24</sup> However, compared to selenosulfate, selenourea is expensive and not readily available. The selenosulfate methods require long reaction times and/or special instrument to synthesize the nanoparticles because of the presence of a complexant in the reaction media.<sup>7,12</sup> Wang *et al.*<sup>25,26</sup> have reported a milder synthetic route to CdSe using selenides ion, Se<sup>2–</sup> in an autoclave at 80–100 °C and also at room temperature. The reaction was carried out in an organic solvent with KBH<sub>4</sub> as reducing agent.

In this paper, we report a novel facile solution based synthesis of nearly monodispersed CdSe nanoparticles whereby selenium powder is first reacted with sodium borohydride (NaBH<sub>4</sub>) in water to produce selenide ions, which act as the source of selenium, followed by the addition of cadmium chloride. The resultant CdSe is dispersed in tri-*n*-octylphosphine (TOP) and this CdSe–TOP mixture is thermolysed in TOPO or HDA to passivate the surface. The results of the characterization by room-temperature optical absorption and luminescence, IR spectroscopy, X-ray diffraction, transmission electron spectroscopy and energy dispersive spectroscopy are presented and discussed.

## Experimental

### Chemicals

Cadmium chloride, sodium borohydride (NaBH<sub>4</sub>), deionised water (HPLC grade), methanol, toluene, hexadecylamine

Department of Chemistry, University of Zululand, Private Bag X1001, Kwalangezwa, 3886, South Africa

† Electronic supplementary information (ESI) available: IR spectra of HDA- and TOPO-capped CdSe nanoparticles. See DOI: 10.1039/b801717d

(HDA), tri-*n*-octylphosphine (TOP) and tri-*n*-octylphosphine oxide (TOPO technical grade 90%) were purchased from Aldrich. Selenium powder was purchased from Merck. All the chemicals were used as purchased.

### Synthesis of CdSe nanoparticles

In a typical room temperature reaction, 0.63 mmol of selenium powder was mixed with 40 mL of deionised water in a three-necked flask. 1.59 mmol of NaBH<sub>4</sub> was carefully added to this mixture and the flask was immediately purged with nitrogen gas to facilitate an inert atmosphere. After 6 h, 0.63 mmol of CdCl<sub>2</sub> dissolved in 40 mL of deionised water was added to the colorless selenium ion solution to give a wine red solution. The solution was stirred for 30 minutes followed by the addition of excess methanol. The resultant solution was then centrifuged. The CdSe produced was dispersed in TOP and stirred continuously to form a TOP–CdSe solution, which was then injected into hot hexadecylamine at 180 °C in an inert atmosphere. A sudden decrease in temperature was observed. The temperature was then gradually raised to 180 °C and the reaction was allowed to continue for 30 minutes. The reddish brown solution obtained was cooled to 70 °C. Addition of excess anhydrous methanol to the solution resulted in the reversible flocculation of the nanoparticles. The flocculate was separated from the supernatant by centrifugation. Excess methanol was removed under vacuum to give HDA-capped CdSe nanoparticles. The resultant particles were dissolved in toluene to give an optically reddish brown solution of nanocrystallites for characterization.

The process was repeated for the TOPO-capped CdSe nanoparticles with TOPO replacing the HDA. The injection temperature was 250 °C. The color of the TOPO-capped CdSe solution was more intense than the HDA-capped CdSe.

All measurements shown in this paper were performed without any post preparative size separation of nanocrystals.

### Optical characterization

A Perkin Elmer Lambda 20 UV-Vis Spectrophotometer was used to carry out optical measurements in the 200–1100 nm wavelength range at room temperature. Samples were placed in quartz cuvettes (1 cm path length). Infrared spectra were carried out using Perkin Elmer Paragon 1000 FT-IR Spectrometer as KBr pellets.

Room-temperature photoluminescence (PL) spectra were recorded on a Perkin Elmer LS 55 luminescence spectrometer with Xenon lamp over 400–800 nm range. The samples were placed in quartz cuvettes (1 cm path length). The wavelength of excitation is indicated in the text and was shorter than the onset of absorption of the sample being studied.

### X-Ray powder diffraction

Samples were mounted on glass capillaries in lacquer droplets roughly 0.8 mm in diameter. Powder diffraction patterns were recorded on an Oxford Xcalibur 2 four-circle diffractometer (CCD detector) using Mo-K $\alpha$  radiation ( $\lambda = 0.71703$  Å). The data were collected and averaged over three runs at  $2\theta = 0, 90$  and  $180^\circ$  with 30 s exposures at an X-ray power of 2.0 kW. The temperature was 100(2) K.

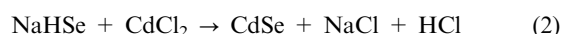
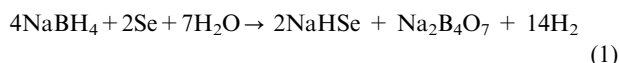
### Transmission electron microscopy

Samples for analysis were prepared by putting an aliquot of a toluene solution of the nanocrystalline material onto an amorphous carbon substrate supported on a copper grid and then allowing the solvent to evaporate at room temperature. A Philips CM120 BIOTWIW transmission electroscop sample viewed at 80 k was used for TEM.

## Results and discussion

### Synthetic method

The method employed in this study is a modification of Rao *et al.*<sup>27</sup> who prepared t-selenium nanorods and nanowires in water using selenide ion (Se<sup>2-</sup>) as the source of selenium. In our reaction, colloidal CdSe nanoparticles have been synthesized by the addition of an aqueous cadmium chloride solution to a freshly prepared oxygen-free NaHSe. The sequence of reactions is shown in eqn (1) and eqn (2):



The CdSe particles are dispersed in TOP and thermolysed in high boiling point coordinating solvents, TOPO and HDA which have been previously successfully used as capping groups, which give higher surface passivation due to greater coverage of the coordinately unsaturated Cd at the surface by the ligands.<sup>13,18,28–30</sup> The stability of the TOPO-capped particles is due to the high affinity of TOPO for Cd<sup>2+</sup> and its bulky nature also provides increased steric hindrance.<sup>28,31</sup> In contrast HDA a primary amine is a slightly weaker base than TOPO, with less steric hindrance creating a larger capping density. The resultant increased surface passivation leads to higher photoluminescence efficiency of the nanoparticles.<sup>18,29</sup>

### UV-Vis absorption spectra

The spectroscopic monitoring of CdSe nanoparticles is a very good example of band-gap engineering. The band gap of CdSe can be tuned across a large portion of the visible spectrum by varying the size of the particles. The UV-absorption spectra for the as-prepared HDA- and TOPO-capped CdSe nanoparticles are shown in Fig. 1. The absorption band edge as calculated using the direct band gap method<sup>32</sup> are 2.09 eV (593 nm, HDA) and 2.03 eV (618 nm, TOPO), both blue-shifted in relation to bulk CdSe, 1.73 eV (716 nm). The UV spectra also show distinct excitonic features at 2.20 eV (563 nm, HDA) and 2.15 eV (576 nm, TOPO) which can be attributed to the first electronic transition (1s–1s) occurring in CdSe nanoparticles.<sup>28,33</sup> The excitonic shoulder and sharp absorption edge is indicative of particles with a narrow size distribution. The sizes of the CdSe particles as calculated from the excitonic peak using Yu's calibration data equation<sup>34</sup> are 3.3 nm (HDA capped) and 3.7 nm (TOPO capped). Similar results were obtained using the effective mass approximation (EMA) model and UV/Vis calibration curves published by Murray *et al.*<sup>13</sup> The slight increase in the size of the TOPO-capped CdSe particles as compared to the HDA-capped

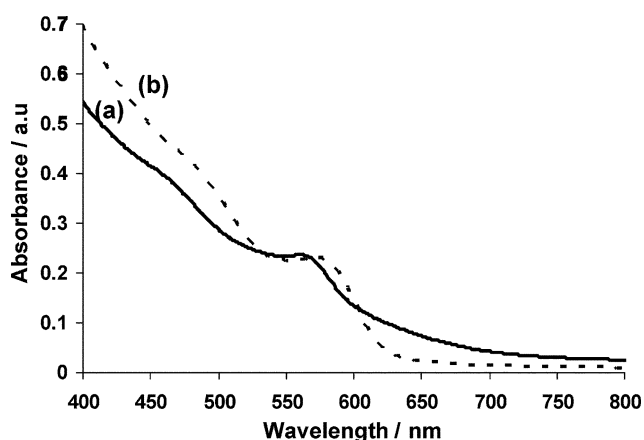


Fig. 1 Absorption spectra of (a) HDA- and (b) TOPO-capped CdSe.

particles has been reported previously for CdSe by Talapin *et al.*<sup>35</sup> The authors attributed the difference in sizes to the redistribution of electronic density in the semiconductor core under the influence of passivating groups or loss of surface Cd and Se atoms with leaving TOPO molecules.

### Photoluminescence spectra

The photoluminescence spectra for both the HDA and TOPO-capped particles exhibit band-edge luminescence for excitation at 400 nm (Fig. 2). The emission peaks are narrow confirming the monodispersity of the particles and the emission maxima show a red shift in relation to the corresponding absorption band-edge. The narrow emission line width indicates the growth of the crystallites with few electronic defect sites. The sharp luminescence shows the efficiency of the capping group in electronically passivating the surface states or defects which are normally associated with semiconductor nanoparticles. The as-prepared samples still show strong emission after about one year of storage. The enhancement of the band edge PL in HDA in comparison with TOPO-capped CdSe nanocrystals can be attributed to the strong bonding of the amines to the nanocrystal surface, which enhances passivation. Less sterically hindered amines may improve surface capping and, hence, passivation of traps by creating a larger capping density.<sup>18,36</sup> In order to check the purity of the sample, photoluminescence spectra of the nanoparticles were mea-

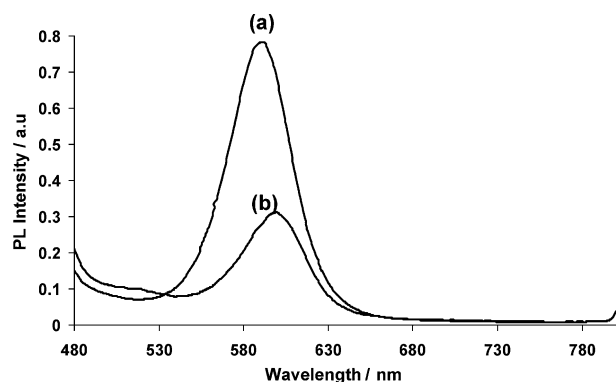


Fig. 2 Photoluminescence spectra ( $\lambda_{400}$  nm) of (a) HDA- and (b) TOPO-capped CdSe.

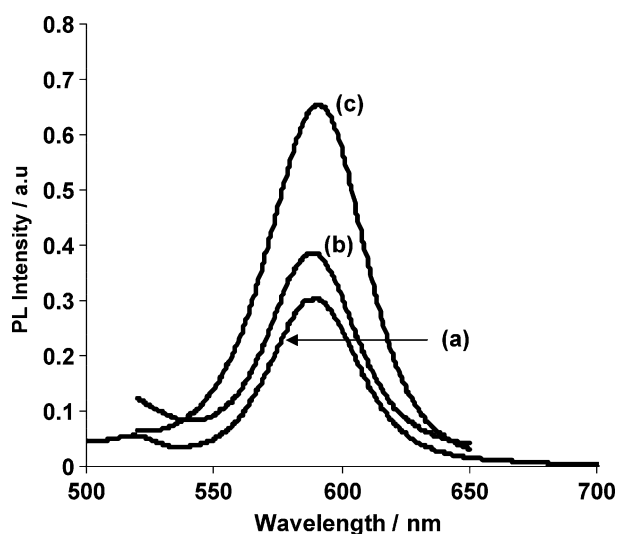
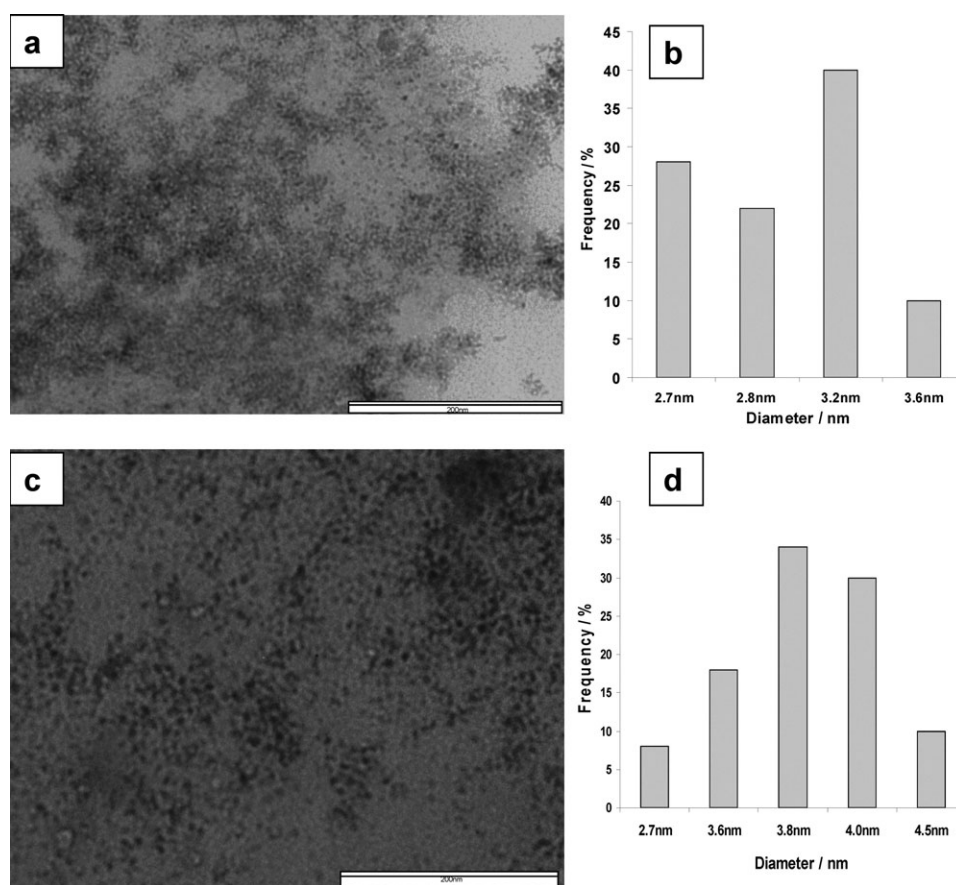


Fig. 3 Photoluminescence spectra of HDA-capped CdSe at different excitation wavelengths, (a) 350 nm, (b) 400 nm, (c) 480 nm.

sured with several excitation wavelengths from 350 to 480 nm (Fig. 3). While the fluorescence intensity changes with excitation wavelength, the fluorescence peak position remained unchanged. This indicates that the fluorescence involves the same initial and final state even though the excitation wavelength was varied between 350 and 450 nm, suggesting fast relaxation from the final state reached by photo excitation to the states from which the fluorescence originates.<sup>37</sup> This lack of wavelength dependence of the fluorescence peak implies that there is only one emitting species in the sample. In other words the samples do not contain any impurities such as unreactive cadmium, or selenium. This observation has also been reported by Banin and co-workers<sup>38</sup> and has been attributed as a strong evidence for the purity of the samples.

### XRD and TEM analysis

The TEM images (Fig. 4) of the as-prepared CdSe particles show well-defined, monodispersed, spherical particles. The average particle sizes as calculated from the TEM images are  $3.0 \pm 0.3$  nm and  $3.8 \pm 0.4$  nm for the respective HDA- and TOPO-capped CdSe particles. These particle sizes corroborates the sizes calculated using the optical measurements. The crystallinity of the particles was probed by X-ray diffraction. CdSe particles can exist as either the cubic or hexagonal phase. The existence of a mixture of cubic and hexagonal phase with the predominance of one over the other is a possibility as reported by Bawendi *et al.*<sup>39</sup> Fig. 5 and Fig. 6 show the wide angle X-ray diffraction patterns of the prepared CdSe nanocrystals. The broad nature of the XRD peaks could be attributed to the nanocrystalline nature of the CdSe particles, which is consistent with the results from the optical analysis. The XRD pattern of the HDA-capped CdSe nanocrystals shows five distinct diffraction peaks at  $2\theta$  values of 23.3, 32.1, 38.3, 41.2 and 44.8°, respectively, corresponding to the (002), (102), (110), (103) and (112) crystalline planes of hexagonal CdSe. The stronger and narrower (002) peak in Fig. 5 indicates that the nanocrystals were elongated along the



**Fig. 4** (a) TEM images of HDA-capped CdSe and (b) corresponding size distribution; (c) TEM images of TOPO-capped CdSe and (d) corresponding size distribution.

*c*-axis. The XRD pattern of the TOPO-capped CdSe nanocrystals shows four diffraction peaks corresponding to the (111), (200), (220) and (311) crystalline planes of cubic CdSe. The synthesis of cubic CdSe at these reaction conditions (high temperature in TOPO) is not well documented. The thermodynamically-stable wurtzite phase is achieved at higher temperature, at which thermodynamics (rather than the reaction kinetics) govern the crystal growth and for the kinetically stable zinc-blende cubic phase the reverse is the case.<sup>13,40,41</sup> In this work it is likely that the preparatory route for the

synthesis of the CdSe nanocrystallites before passivation and the variation of the capping agent could be responsible for the change in the crystal structure.

### IR spectroscopy

The surface morphology of the CdSe was investigated by IR spectroscopy, to confirm the capping of the particles by the passivating agent. TOPO absorbs strongly at 1466 and

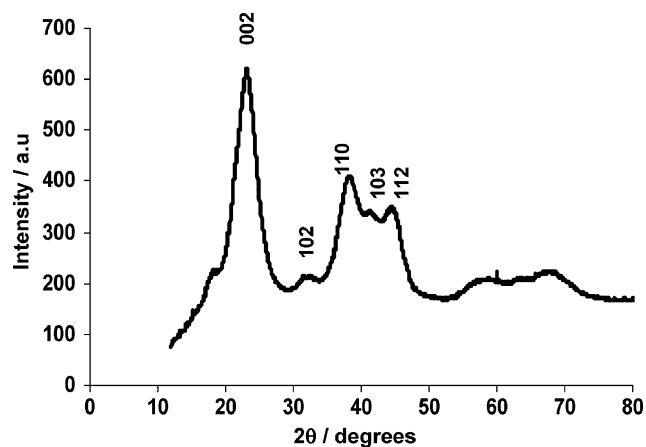


**Fig. 5** XRD pattern of HDA-capped CdSe nanoparticles.

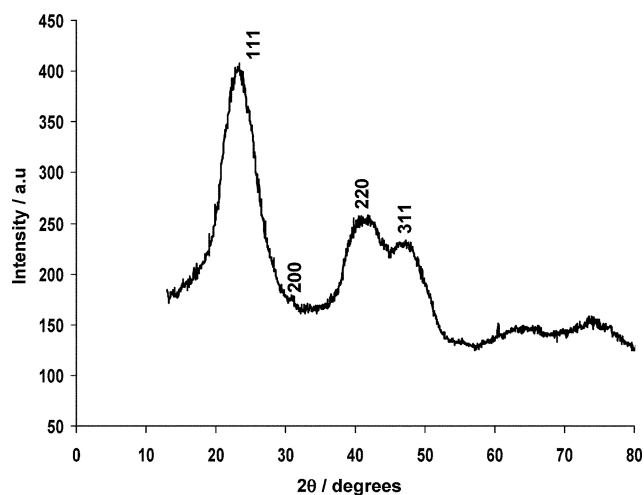


**Fig. 6** XRD pattern of TOPO-capped CdSe nanoparticles.

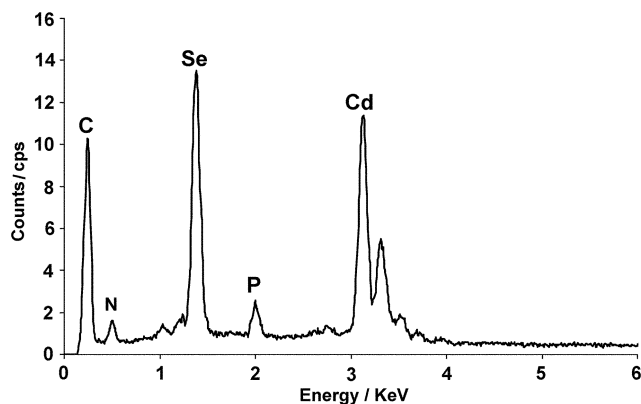
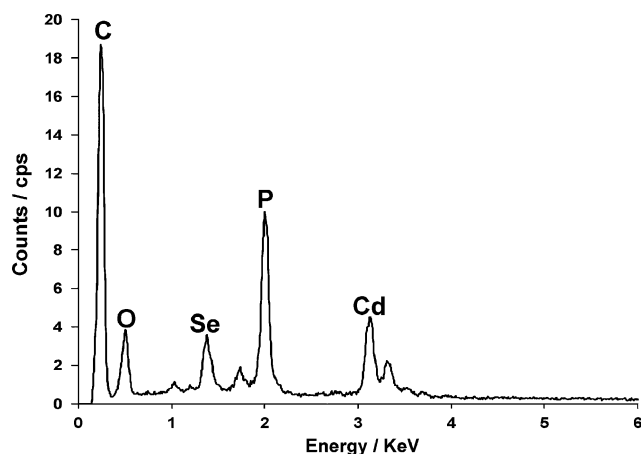


**Table 1** Assignment of IR bands for HDA-capped CdSe

HDA	CdSe/HDA	Band
3331 (m)	3334 (w)	N–H str
2954 (m)	2958 (m)	CH <sub>3</sub> (C–H str)
2916 (vs)	2919 (vs)	CH <sub>2</sub> (C–H str)
2847 (vs)	28 519 (vs)	CH <sub>2</sub> (C–H str)
	2676, 2569 (w)	CH <sub>2</sub> (C–H str)
1462 (s)	1470 (s)	CH <sub>2</sub> /CH <sub>3</sub> bend
1363 (m)	1376 (m)	CH <sub>3</sub> bend
1058 (s)	1062 (w)	C–N str
	1176	C–N str
719 (s)	721 (s)	(CH <sub>2</sub> ) <sub>n</sub> rocking
	1400	P–CH <sub>2</sub> bend

m = Medium, w = weak, S = strong, vs = very strong.

1146 cm<sup>-1</sup> corresponding to CH<sub>2</sub> bending and P=O stretching, respectively, the position of which depends on the attached group.<sup>42</sup> In this work a shift of 14 cm<sup>-1</sup> ( $\nu = 1452$  cm<sup>-1</sup>) to lower wavenumbers from the characteristic stretch of TOPO ( $\nu_{\text{sym}}$ , P=O = 1466 cm<sup>-1</sup>) is observed. This shift has been observed previously for TOPO bound CdSe-capped nanoparticles and attributed to the binding of TOPO to Cd<sup>2+</sup> sites on the CdSe nanocrystallites surface.<sup>28</sup> The IR spectrum of HDA-capped CdSe shows bands that are shifted to higher frequencies when compared to the free ligand. The band assignments are given in Table 1. This shift has been reported for amine bound to CdSe and may be due to coordination to the nanocrystallites.<sup>15</sup> The weak bands at 2676 and 2569 cm<sup>-1</sup> appearing in the HDA-capped CdSe as well as C–N stretching band at 1176 cm<sup>-1</sup> are attributed to the coordination of the TOP and the nanocrystallites to the nitrogen atom of the amine. The band at 1400 cm<sup>-1</sup> is assigned to be P–CH<sub>2</sub> bending due to the presence of the phosphine. The presence of phosphorus is also confirmed by the EDS spectra (Fig. 7 and Fig. 8). Each spectrum shows peaks for Cd and Se confirming the production of selenium nanocrystallites. In the case of the HDA-capped particles (Fig. 7) the low intensity of the nitrogen peak is due to suppression from the high intensity of the carbon peak, whose source is the carbon tape used to suspend the powdered samples. The peak near 0.5 keV in Fig. 8 is assigned to O, which is the oxygen atom from the TOPO. The intensity of the phosphorus peak in TOPO-capped CdSe is higher with absence of nitrogen peak as compared to HDA-capped CdSe.

**Fig. 7** EDS spectrum of HDA-capped CdSe nanoparticles.**Fig. 8** EDS spectrum of TOPO-capped CdSe nanoparticles.

## Conclusions

Monodispersed HDA- and TOPO-capped CdSe nanoparticles have been prepared for the first time by a new route using selenide ion (Se<sup>2-</sup>) produced from selenium powder as the selenium source. Optical and structural analysis show that the samples are of high quality and exhibit quantum confinement. Capping of the nanoparticles surface by HDA and TOPO was confirmed by FT-IR and EDS spectroscopy. The synthetic procedure developed here offer several important advantages for the synthesis of selenide nanocrystals. The technique is environmentally friendly, inexpensive, involving the use of relatively non-toxic reagents and has a short reaction time. At present, we are using the synthetic method to synthesize various selenide based nanoparticles and investigating the effect of monomer concentration, addition time of metal salt, temperature, and pH on the size, colour and shape of the selenide nanoparticles.

## Acknowledgements

We thank Olabisi Onabanjo University (O.O.U.) Ago-Iwoye, Nigeria for the opportunity given to S. O. O. to carry out this research at the University of Zululand. We acknowledge the CSIR and National Research Foundation (NRF), South Africa for financial support. We also thank center for electron microscopy (UKZN) for TEM measurements.

## References

1. R. Coustal, *J. Chem. Phys.*, 1958, **38**, 277.
2. H. C. Yi and J. J. Moore, *J. Mater. Sci.*, 1990, **25**, 1159.
3. I. P. Parkin, *Chem. Soc. Rev.*, 1996, **25**, 199.
4. H. C. Metcalf, J. E. Williams and J. F. Caska, *Modern Chemistry*, Holt, Reinhart & Winston, New York, 1982, pp. 454.
5. D. S. Xu, X. S. Shi, G. L. Guo, L. Gui and Y. Q. Tang, *J. Phys. Chem. B*, 2000, **104**, 5061.
6. J. Zhu, Y. Koltypin and A. Gedanken, *Chem. Mater.*, 2000, **12**, 73.
7. J. Zhu, O. Palchik, S. Chen and A. Gedanken, *J. Phys. Chem. B*, 2000, **104**, 7344.
8. Y. Wang, Z. Tang, M. A. Correa-Duarte, I. Pastorizanto, M. Giersig, N. A. Kotov and L. M. Liz-Marzan, *J. Phys. Chem. B*, 2004, **108**, 15461.
9. S. Gorer, A. Albu-Yaron and G. Hodes, *Chem. Mater.*, 1995, **7**, 1243.

10. O. Yamamoto, T. Sasamoto and M. Inagaki, *J. Mater. Res.*, 1998, **13**, 3394.
11. D. V. Das and K. S. Bhat, *J. Mater. Sci.*, 1990, **1**, 1.
12. W. Zaho, J. Zhu and H. Chen, *J. Cryst. Growth*, 2003, **252**, 587.
13. C. B. Murray, D. J. Norris and M. G. Bawendi, *J. Am. Chem. Soc.*, 1993, **115**, 8706.
14. T. Trindade and P. O'Brien, *Adv. Mater.*, 1996, **8**, 161.
15. T. Trindade, P. O'Brien and X. Zhang, *Chem. Mater.*, 1997, **9**, 523.
16. B. Ludolph, M. A. Malik, P. O'Brien and N. Revaprasadu, *Chem. Commun.*, 1998, 1849.
17. M. Chunggaze, J. M. Aleese, P. O'Brien and D. J. Otway, *Chem. Commun.*, 1998, 833.
18. M. A. Hines and P. Guyot-Sionnest, *J. Phys. Chem. B*, 1998, **102**, 3655.
19. N. Revaprasadu, M. A. Malik, P. O'Brien, M. M. Zulu and G. Wakefield, *J. Mater. Chem.*, 1998, **8**, 1885.
20. P. K. Khanna, R. M. Gorte and R. Gokhale, *Mater. Lett.*, 2004, **58**, 966.
21. X. Chen, Y. Lou and C. Burda, *Int. J. Nanotechnol.*, 2004, **1**, 105.
22. Z. A. Peng and X. G. Peng, *J. Am. Chem. Soc.*, 2001, **123**, 183.
23. M. A. Malik, N. Revaprasadu and P. O'Brien, *Chem. Mater.*, 2001, **13**, 913.
24. Y. J. Yang and B. J. Xiang, *J. Cryst. Growth*, 2005, **284**, 453.
25. W. Wang, Y. Geng, P. Yan, F. Liu, Y. Xie and Y. Qian, *Inorg. Chem. Commun.*, 1999, **2**, 83.
26. W. Wang, Y. Geng, P. Yan, F. Liu, Y. Xie and Y. Qian, *J. Am. Chem. Soc.*, 1999, **121**, 4062.
27. U. K. Gautam, M. Nath and C. N. R. Rao, *J. Mater. Chem.*, 2003, **13**, 2845.
28. J. E. Bowen-Katari, V. L. Colvin and A. P. Alivisatos, *J. Phys. Chem.*, 1994, **98**, 4109.
29. L. Qu and X. Peng, *J. Am. Chem. Soc.*, 2002, **124**, 2049.
30. J. A. Gaunt, A. E. Knight, S. A. Windsor and V. Chechik, *J. Colloid Interface Sci.*, 2005, **290**, 43.
31. K. Satoh, Y. Takahashi, T. Suzuki and K. Sawada, *J. Chem. Soc., Dalton Trans.*, 1989, 259.
32. J. L. Pankove, *Optical Processes in Semiconductors*, Dover Publications, New York, 1990.
33. M. G. Bawendi, M. L. Steigerwald and L. E. Brus, *Annu. Rev. Phys. Chem.*, 1990, **41**, 477.
34. W. W. Yu, L. Qu, W. Guo and X. Peng, *Chem. Mater.*, 2003, **15**, 2854.
35. D. V. Talapin, A. L. Rogach, A. Kornowski, M. Haase and H. Weller, *Nano Lett.*, 2001, **1**, 207.
36. X. Peng, M. C. Schlamp, A. Kadavanich and A. P. Alivisatos, *J. Am. Chem. Soc.*, 1997, **119**, 9869.
37. J. Joo, H. B. Na, T. Yu, Y. W. Kim, F. Wu, J. Z. Zhang and T. Hyeon, *J. Am. Chem. Soc.*, 2003, **125**, 11100.
38. V. N. Soloviev, A. Eichhofer, D. Fenske and U. Banin, *J. Am. Chem. Soc.*, 2001, **123**, 2354.
39. M. G. Bawendi, A. R. Kortan, M. L. Steigerwald and L. E. Brus, *J. Chem. Phys.*, 1989, **91**, 7282.
40. Q. Lianhua, Z. A. Peng and X. Peng, *Nano Lett.*, 2001, **1**, 333.
41. T. Vossmeier, L. Katsikas, M. Giersig, L. G. Popovic, K. Diesner, A. Chemseddine, A. Eychmuller and H. Weller, *J. Phys. Chem.*, 1994, **98**, 7665.
42. N. B. Colthup, L. H. Daly and S. E. Wiberley, *Introduction to Infrared and Raman Spectroscopy*, Academic Press, Inc., San Diego, 3rd edn, 1990, pp. 364.